Molecular Biology of the Cell
Vol. 8, 973–985, June 1997

Nanomolar Concentrations of Nocodazole Alter Microtubule Dynamic Instability In Vivo and In Vitro

Robert J. Vasquez,*† Bonnie Howell,* Anne-Marie C. Yvon,‡ Patricia Wadsworth,‡ and Lynne Cassimeris*§

*Department of Biological Sciences, Lehigh University, Bethlehem, Pennsylvania 18015; and
‡Department of Biology and Program in Molecular and Cellular Biology, University of Massachusetts, Amherst, Massachusetts 01003

Submitted November 20, 1996; Accepted March 5, 1997
Monitoring Editor: Marc Kirschner

Previous studies demonstrated that nanomolar concentrations of nocodazole can block cells in mitosis without net microtubule disassembly and resulted in the hypothesis that this block was due to a nocodazole-induced stabilization of microtubules. We tested this hypothesis by examining the effects of nanomolar concentrations of nocodazole on microtubule dynamic instability in interphase cells and in vitro with purified brain tubulin. Newt lung epithelial cell microtubules were visualized by video-enhanced differential interference contrast microscopy and cells were perfused with solutions of nocodazole ranging in concentration from 4 to 400 nM. Microtubules showed a loss of the two-state behavior typical of dynamic instability as evidenced by the addition of a third state where they exhibited little net change in length (a paused state). Nocodazole perfusion also resulted in slower elongation and shortening velocities, increased catastrophe, and an overall decrease in microtubule turnover. Experiments performed on BSC-1 cells that were microinjected with rhodamine-labeled tubulin, incubated in nocodazole for 1 h, and visualized by using low-light–level fluorescence microscopy showed similar results except that nocodazole-treated BSC-1 cells showed a decrease in catastrophe. To gain insight into possible mechanisms responsible for changes in dynamic instability, we examined the effects of 4 nM to 12 μM nocodazole on the assembly of purified tubulin from axoneme seeds. At both microtubule plus and minus ends, perfusion with nocodazole resulted in a dose-dependent decrease in elongation and shortening velocities, increase in pause duration and catastrophe frequency, and decrease in rescue frequency. These effects, which result in an overall decrease in microtubule turnover after nocodazole treatment, suggest that the mitotic block observed is due to a reduction in microtubule dynamic turnover. In addition, the in vitro results are similar to the effects of increasing concentrations of GDP-tubulin (TuD) subunits on microtubule assembly. Given that nocodazole increases tubulin GTPase activity, we propose that nocodazole acts by generating TuD subunits that then alter dynamic instability.

INTRODUCTION

Microtubules (MTs) are linear protein polymers that play a role in many structural and motile phenomena in the cell, including the movement of vesicles and organelles, the establishment of Golgi and endoplasmic reticulum membrane systems (reviewed in Cole and Lippincott-Schwartz, 1995) and the movement of chromosomes during mitosis (reviewed in Inoue and Salmon, 1995). MT behavior is characterized by a phenomenon called dynamic instability (Mitchison and Kirschner, 1984a,b; Walker *et al.*, 1988; reviewed in Erickson and O'Brien, 1992; Cassimeris, 1993), where

† Present address: Department of Cell Biology, Worcester Foundation for Biomedical Research, Worcester, MA 01545.
§ Corresponding author: Department of Biological Sciences, 111 Research Drive, Lehigh University, Bethlehem, PA 18015.

MTs exist in one of two persistent phases, elongation or rapid shortening, with abrupt and apparently random transitions between these two states. The switch from elongation to shortening is termed catastrophe, and the switch from shortening to elongation is termed rescue (Walker *et al.*, 1988). It appears that it is the presence or absence of a GTP-tubulin (TuT) cap (or GDP-Pi tubulin cap) at the MT ends that determines the assembly state of an individual MT (Carlier *et al.*, 1987; Melki *et al.*, 1990; reviewed in Caplow, 1992; Erikson and O'Brien, 1992; Hyman *et al.*, 1992; Drechsel and Kirschner, 1994; Caplow and Shanks, 1996).

MT drugs are valuable tools with which to probe the assembly dynamics of MTs and to potentially uncover mechanisms that regulate MT dynamic instability (Wilson and Jordan, 1995). One such drug, nocodazole, a benzimidazole derivative, was initially developed as a potential anticancer drug. It is still widely used to study MT-dependent processes because of its ability to rapidly depolymerize MTs in vivo when administered at micromolar concentrations. Early studies demonstrated that, at concentrations equal to or greater than those of tubulin, nocodazole inhibits tubulin polymerization in vitro (Hoebeke *et al.*, 1976; Friedman and Platzer, 1978; Ireland, 1979; Lee *et al.*, 1980) and in vivo (DeBrabander *et al.*, 1976). Cultured cells treated with high concentrations of nocodazole quickly depolymerize their MTs and are prevented from proceeding through mitosis (DeBrabander *et al.*, 1976). Other studies have demonstrated that nocodazole competes with colchicine for tubulin binding but that nocodazole exhibits more rapid binding to, and dissociation from, tubulin than does colchicine (Hoebeke, 1976; Lee *et al.*, 1980).

Recent studies of several MT drugs indicate that, at low concentrations relative to tubulin, these drugs can disrupt MT-dependent processes by altering MT dynamics, without resulting in significant MT depolymerization (Jordan and Wilson, 1990; Jordan *et al.*, 1992; Toso *et al.*, 1993; Dhamodharan *et al.*, 1995; Tanaka *et al.*, 1995). For example, Jordan *et al.* (1992) found that at relatively low concentrations, vinblastine, podophyllotoxin, and nocodazole induce mitotic arrest without significant changes in MT polymer level. More detailed studies of vinblastine have indicated that this drug alters dynamic instability by binding to high-affinity sites near the ends of MTs, thereby slowing the addition and loss of subunits from the MT end (Jordan and Wilson, 1990; Jordan *et al.*, 1991; Toso *et al.*, 1993). In a recent study, Dhamodharan *et al.* (1995) found that nanomolar concentrations of vinblastine effectively suppress the dynamics of individual MTs in cultured cells at concentrations of the drug that do not result in significant changes in MT polymer mass. Other studies with low concentrations of taxol, a drug that induces MT polymer assembly, also indicate that at low concentrations, mitotic arrest occurs due to reduction or elimination of MT dynamic instability rather than a gross change in MT polymer (Jordan *et al.*, 1993).

In light of these recent studies of MT drugs, we examined the effects of low concentrations of nocodazole on the dynamic instability of individual MTs in living cells and in vitro to test the hypothesis that low concentrations of nocodazole block cells in mitosis by stabilizing MTs (Jordan *et al.*, 1992). We find that nanomolar concentrations of nocodazole significantly reduce the growth and shortening velocities of dynamic instability and increase the time that MTs spend in a paused or attenuated state. We propose a mechanism involving increased GTP hydrolysis by tubulin dimers to explain these results and suggest that cells are likely to contain endogenous molecules that regulate MT turnover by similar mechanisms.

MATERIALS AND METHODS

Stock Solutions and Protein Purification

Nocodazole was purchased from Sigma (St. Louis, MO) and prepared as a stock concentration of 33.3 mM in dimethyl sulfoxide. Aliquots were kept at −20°C and diluted to final concentrations in PEM buffer [0.1 M piperazine-*N*,*N*′-bis(2-ethanesulfonic acid), pH 6.9, 2 mM EGTA, 1 mM $MgSO_4$] for in vitro studies or in cell culture medium for in vivo studies. These working dilutions were kept on ice and used within 4 h to minimize the likelihood of the nocodazole precipitating out of solution (Lee *et al.*, 1980).

Porcine brain tubulin and axoneme fragments from *Strongylocentrotus purpuratus* sperm were prepared as described previously (Vasquez, *et al.* 1994). No microtubule-associated proteins were detectable in the three-time–cycled, phosphocellulose-purified, and glutamate-cycled tubulin by silver staining (Morrisey, 1981) of overloaded SDS-PAGE minigels (50 μg/lane; Walker *et al.*, 1988).

Rhodamine-labeled tubulin was prepared as described in Dhamodharan and Wadsworth (1995) as modified from Hyman *et al.* (1991) and Vigers *et al.* (1988). Briefly, phosphocellulose-purified brain tubulin was assembled in PEM buffer containing 4 M glycerol at 37°C for 30 min and labeled with a 40-fold molar excess of 5,6-carboxysuccinamidyl ester of rhodamine (Molecular Probes, Eugene, OR). The MT polymer was sedimented at 200,000 × *g* for 2 h at 25°C and subjected to three rounds of assembly and disassembly in glutamate buffer (1 M sodium glutamate, 0.5 mM $MgSO_4$, 1.0 mM EGTA, 1.0 mM GTP, pH 6.9) to remove unbound dye and inactive tubulin (Wadsworth and Salmon, 1986). The final pellet of MTs was resuspended in microinjection buffer (20 mM glutamate, 0.5 mM $MgSO_4$, 1.0 mM EGTA, pH 7.2), clarified by brief centrifugation, distributed into aliquots, drop-frozen in liquid nitrogen, and stored at −80°C.

Cell Culture

Primary cultures of newt lung epithelial cells were grown on coverslips as described by Rose *et al.* (1958) in chambers at room temperature (23°C) as described previously (Cassimeris *et al.*, 1988). Cells were maintained in half-strength L-15 medium (pH 7.2) supplemented with 10% fetal bovine serum, 5 mM HEPES buffer, 100 U/ml penicillin, 0.1 mg/ml streptomycin, and 0.25 μg/ml amphotericin B. BSC-1 cells were cultured and grown on coverslips as described previously (Shelden and Wadsworth, 1993; Dhamodharan *et al.*, 1995).

In Vivo MT Assembly Assays

Individual MTs in the flat peripheral regions of newt lung epithelial cells were followed with video-enhanced differential interference contrast light microscopy (VE-DIC; Cassimeris *et al.*, 1988). Dynamic MTs were followed for 2 to 5 min before and after perfusion with 4, 100, or 400 nM nocodazole, diluted in culture medium. Culture medium was warmed to 23°C prior to perfusion. These experiments were conducted at 23°C.

BSC-1 cells were injected with rhodamine-labeled tubulin as described previously (Shelden and Wadsworth, 1993). The cells were then incubated for 1 to 3 h at 37°C to allow incorporation of the labeled tubulin into MTs. After incubation, the culture medium was replaced with medium containing the appropriate concentration of nocodazole (4, 100, or 500 nM) and incubated at 37°C for an additional 1 h prior to observation of MTs. Additional perfusion experiments, similar to those described for newt lung cells, were performed at 100 nM nocodazole. MTs were followed for 2 to 16 min after perfusion.

In Vitro Assembly Assays

The assembly of individual MTs seeded from axonemes was observed with VE-DIC as described previously (Vasquez *et al.*, 1994). Briefly, axonemes were allowed to adhere to biologically clean coverslips for ~5 min in a humid chamber. The coverslips were then mounted onto clean glass slides with strips of parafilm serving as spacers, creating ~50-μl chambers. Tubulin, diluted to the appropriate concentration in PEM buffer containing 1 mM GTP, was loaded into the chamber, two sides of the chamber were sealed with VALAP (1:1:1 mixture of Vaseline, lanolin, and petrolatum), and assembly was followed by VE-DIC, with digital image processing, at 35°C, using an air curtain incubator (Nickolson Precision Instruments, Gaithersburg, MD) to maintain temperature. After assembly had occurred for several minutes, a solution of nocodazole, tubulin, and GTP, briefly warmed in a 37°C water bath, was perfused through the chamber. There was a short window of time (typically 20–45 s) before focus was restored. For the experiments shown in Figure 5, a second person maintained focus while the first person perfused solutions, this decreased the time microtubules were out of focus. Real-time images were collected on Super-VHS videotape throughout experiments.

Microscopy and Image Acquisition

DIC Microscopy. The system used for VE-DIC microscopy consisted of a Nikon microphot-SA equipped with 60× 1.4 numerical aperature (NA) PlanApo lens, DIC prisms, and a 1.4 NA condenser. Illumination was provided by a 100-W mercury lamp passed through an Ellis light scrambler (Technical Video, Woods Hole, MA). The microscope was also equipped with heat-absorbing and 546-nm interference filters. Images were projected through a 5× projection lens to a 2400 Newvicon video camera (Hammamatsu, Bridgewater, NJ). Images were further enhanced with an Argus 10 image processor (Hamamatsu) for real-time two- or four-frame exponential averaging. After passage through a time date generator (For-A, Natick, MA), images were recorded onto super-VHS video tapes with a Sony SV0–9500 MD recorder.

Fluorescence Microscopy. Microscopic analysis of rhodamine-labeled MTs in BSC-1 cells was performed as described in Dhamodharan and Wadsworth (1995) and Shelden and Wadsworth (1993). Cultures containing microinjected cells were placed into chambers (Rose *et al.*, 1958) and observed with a Zeiss IM-35 inverted microscope that was maintained at 36 ± 1°C by an air curtain incubator (Nicholson Precision Instruments). Peripheral regions of the cells were imaged with a Nikon 100× 1.3 NA objective, and images (32 frame averages) were collected at 2-s intervals with a DAGE-ISIT video camera and digitized with a Perceptics PixelPipeline card in a Macintosh Quadra 950 computer running BDS Image (Oncor, Gaithersburg, MD) software. Images were stored on optical discs.

MT Tracking and Analysis of Dynamics

For data collected by VE-DIC, the rates of MT elongation and shortening were determined from video tapes with software designed by Salmon and colleagues (Gliksman *et al.*, 1992). This program plots changes in MT length as a function of time, creating MT life histories. The elongation and shortening rates were calculated from the slopes of length versus time plots by a least squares regression analysis. For the in vitro assembly assays, plus and minus ends were assigned based on MT elongation velocities prior to nocodazole addition. For BSC-1 cells, analysis of MT dynamics was performed as described in detail in Dhamodharan and Wadsworth (1995). For all velocity data, values are reported as the mean ± SE (where SEM = SD/$\sqrt{n}$).

From these life-history plots, transition frequencies were calculated as described previously (Walker *et al.*, 1988; Vasquez *et al.*, 1994). Briefly, for all MTs of a given polarity, catastrophe frequency (defined as the switch from growth or pause to shortening; Shelden and Wadsworth, 1993; Toso *et al.*, 1993) was calculated by dividing the number of catastrophes observed by the sum of the total time spent in elongation or pause (Walker *et al.*, 1988; Toso *et al.*, 1993). Rescue was defined as a switch from shortening to pause or elongation, and rescue frequency was calculated by dividing the number of rescues observed by the sum of the total time spent in shortening. Standard deviations for transition frequencies were determined from the catastrophe or rescue frequency divided by the square root of the number of transitions observed (Walker *et al.*, 1988). This calculation assumes a Poisson distribution of growth or shortening times (Taylor, 1982).

Time spent in pause was determined by dividing the total time spent in a paused state by the total time of observation. For MTs in newt lung cells, a pause was defined as any change in MT length <0.5 μm/min, and for in vitro MTs, a pause was defined as any rate <0.2 μm/min. For BSC-1 cells, a pause was defined as a length change <0.5 μm (see Dhamodharan and Wadsworth, 1995). The different values for newt lung and BSC-1 cells were selected to take into account the differences in the techniques used to collect the data, and the in vitro definition of pause was necessary because of the slow elongation velocity at minus ends. The definition of a pause in each case also represents current limitations of light microscopy (see also Dhamodharan and Wadsworth, 1995). For example, in newt lung cells, the contrast generated by other cellular components limits our ability to accurately follow slow changes in MT length due to small inaccuracies in identifying the position of the MT end.

Dynamicity, an estimate of the number of tubulin subunits exchanged at MT ends was calculated by dividing the sum of the length grown and shortened, based on 1624 dimers/μm, by the total time a particular MT was observed (Toso *et al.*, 1993).

RESULTS

Nocodazole Suppresses MT Dynamic Instability in Interphase Cells

To determine whether the nocodazole-induced mitotic block (Jordan *et al.*, 1992) could be due to changes in the dynamic instability of MTs, we examined the effects of nocodazole on interphase MTs since it is possible to follow individual MTs during this stage of the cell cycle. We first used VE-DIC to follow MTs in newt lung epithelial cells (Cassimeris *et al.*, 1988) before and after perfusion with 4, 100, or 400 nM nocodazole. Figure 1 shows representative life-history plots of a MT in an untreated cell and an MT before and after perfusion with 4, 100, or 400 nM nocodazole. After perfusion with nocodazole, MTs elongated and short-

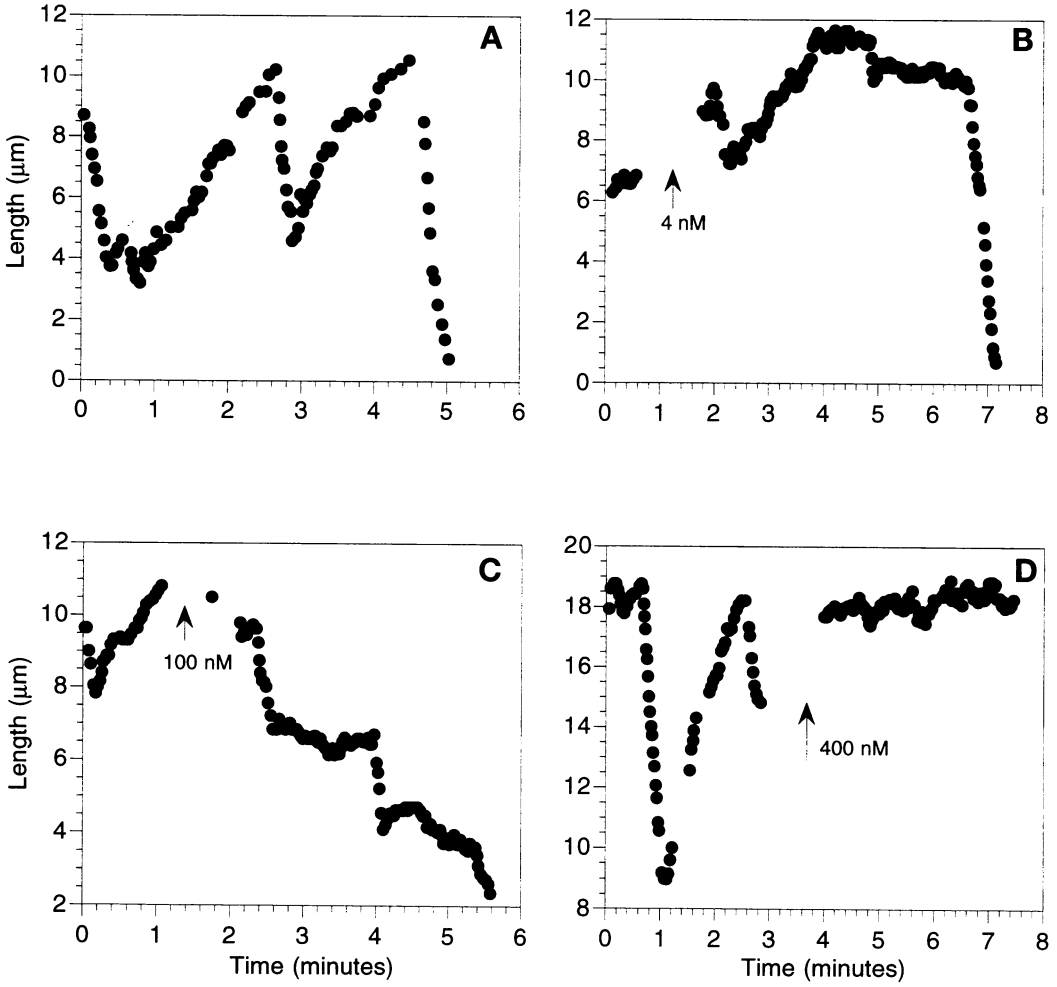

Figure 1. Representative life-history plots of MTs in newt lung epithelial cells from an untreated cell (a) and before and after perfusion with 4, 100, or 400 nM nocodazole (b–d). Arrows, perfusion.

ened more slowly (Table 1). In untreated newt lung cell MTs, the mean elongation velocity was 4.9 μm/min (n = 270; SEM = ±0.14). Perfusion with 100 nM nocodazole decreased the mean elongation velocity to 1.7 μm/min (n = 14; SEM = ±0.25). There also was a reduction in the mean shortening velocity. For exam-

Table 1. MT dynamic instability in newt lung cells treated with nocodazole

Parameter	Untreated	4 nM Noc	100 nM Noc	400 nM Noc
Elongation velocity (μm/min)	4.9 ± 0.14	2.9 ± 0.50	1.7 ± 0.25	2.3 ± 0.21
(n)	(270)	(14)	(14)	(40)
Shortening velocity (μm/min)	14.3 ± 0.6	7.1 ± 1.24	5.1 ± 0.78	4.4 ± 0.51
(n)	(161)	(19)	(34)	(43)
% time in pause	<1	23	42	18
Catastrophe frequency (s^{-1})	0.016 ± 0.001	0.031 ± 0.01	0.034 ± 0.007	0.028 ± 0.005
(n)	(154)	(10)	(24)	(32)
Rescue frequency (s^{-1})	0.052 ± 0.004	0.018 ± 0.006	0.029 ± 0.006	0.043 ± 0.008
(n)	(142)	(8)	(21)	(31)
Dynamicity (dimers/sec)	189.3	153.7	105.2	99.3

Dynamic MTs in newt lung epithelial cells were followed by VE-DIC before and after perfusion with the listed concentrations of nocodazole (Noc). Velocities (mean ± SE), pauses and transition frequencies (average ± SD) were calculated as described in MATERIALS AND METHODS.

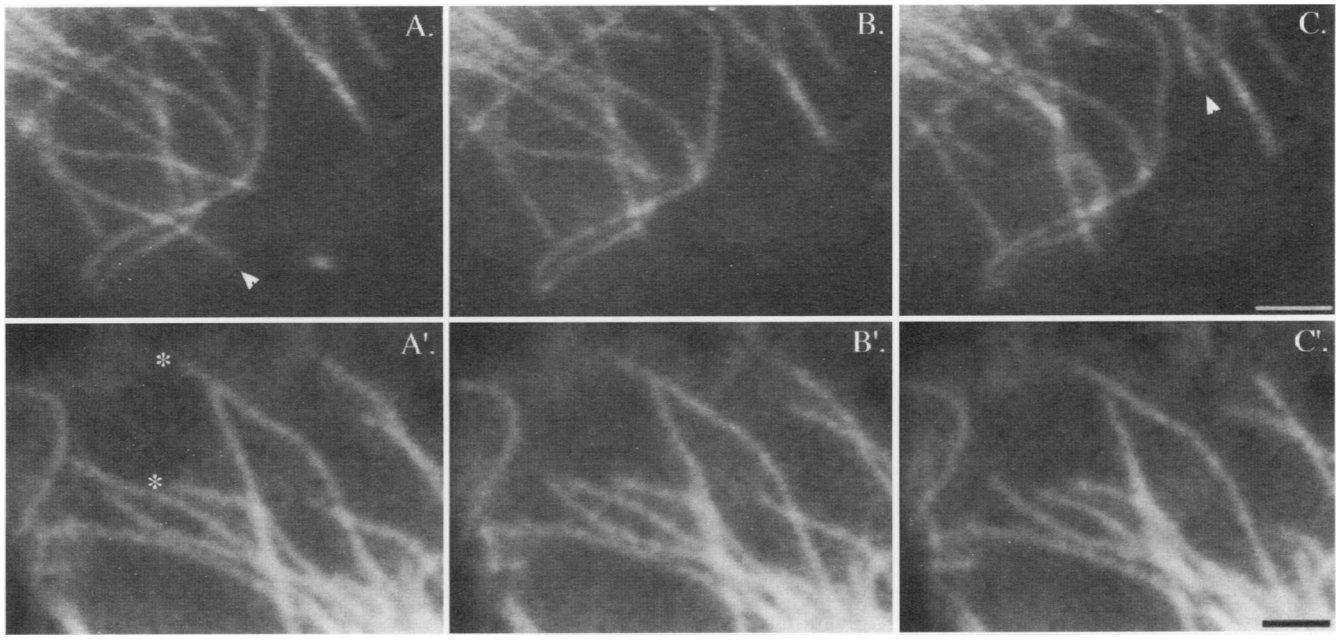

Figure 2. Dynamic behavior of MTs in living BSC-1 cells. Images were collected at 2-s intervals; images shown are 20 s apart. In control cells (A–C), the dynamic behavior of the MTs is apparent, with the MTs both leaving (arrowhead, A) and entering (arrowhead, C) the field of view. In cells treated with 100 nM nocodazole for 1 h (A'–C'), the behavior of the MTs is attenuated; many of the MTs undergo little or no change in length (asterisks in A') over the 40-s interval. Bars, 2 μm.

ple, the mean shortening velocity was reduced from 14.3 μm/min (n = 161; SEM = $\pm$0.6) in untreated cells to 4.5 μm/min (n = 33; SEM = $\pm$0.34) after perfusion with 100 nM nocodazole. Thus, nanomolar concentrations of nocodazole greatly suppressed MT elongation and shortening velocities in newt lung cells.

To expand upon our observations in newt lung cells, we also investigated the effects of nanomolar concentrations of nocodazole in cultured mammalian BSC-1 cells microinjected with rhodamine-labeled tubulin (Figure 2). Unlike the newt lung cell experiments, where nocodazole effects were measured immediately after addition of the drug, BSC-1 cells were incubated for 1 h in nocodazole prior to observation, allowing tubulin and MTs to reach a new intracellular steady state in the presence of the drug. On the basis of qualitative observations, there was little or no change in MT polymer level after 1 h in 4 nM nocodazole, but some loss of polymer was apparent at higher concentrations of the drug based on the higher fluorescence from unincorporated rhodamine tubulin subunits. This result is consistent with quantitative measurements made in HeLa cells incubated for 18 to 20 h in nocodazole, where 100 and 600 nM nocodazole reduced polymer mass by 30% and 50%, respectively (Jordan *et al.*, 1992).

Table 2 provides a summary of the individual parameters of dynamic instability that were measured in BSC-1 cells after 1-h incubations in 4, 100, or 500 nM nocodazole. As in newt lung cells, MTs in BSC-1 cells exhibited reduced elongation and shortening velocities after treatment with nocodazole; growth velocity was reduced from 9.2 μm/min (n = 42; SEM = $\pm$0.76) in untreated cells to 3.0 μm/min (n = 69; SEM = $\pm$0.27) in cells treated with 100 nM nocodazole, whereas shortening velocity drops from 12.4 μm/min (n = 37; SEM = $\pm$1.1) to 4.9 μm/min (n = 66; SEM = $\pm$0.53) under the same conditions. Interestingly, a higher concentration of nocodazole (500 nM) was not as effective in reducing elongation and shortening velocities (Table 2).

The time that MTs spent in a paused state also increased dramatically in both cell types. Pauses are uncharacteristic of the dynamic newt lung cell MTs observed in this and in previous studies (Cassimeris *et al.*, 1988). For the MTs observed in untreated cells, less than 1% of total observed time was spent in pause. After nocodazole perfusion, MTs spent up to 57% of the time observed in pause (Table 1). When MTs exited a paused state, they were more likely to switch to shortening rather than growth. BSC-1 cells also showed a dose-dependent increase in the time spent in a paused state. MTs in untreated cells were in a paused state 45% of the time, and this increased to 85% in cells incubated with 500 nM nocodazole. In contrast to newt lung cells, BSC-1 MTs that exited a paused state showed about equal probabilities of switching to growth or shortening and this was unaffected by nocodazole.

Table 2. MT dynamic instability in BSC cells treated with nocodazole

Parameter	Untreated	4 nM Noc	100 nM Noc	500 nM Noc
Elongation velocity (μm/min)	9.2 ± 0.76	8.0 ± 0.57	3.0 ± 0.27	5.4 ± 0.97
(n)	(42)	(83)	(69)	(19)
Shortening velocity (μm/min)	12.4 ± 1.1	11.8 ± 1.2	4.9 ± 0.53	9.6 ± 2.5
(n)	(37)	(51)	(66)	(13)
% time in pause	45.2	52.4	66.9	85
Catastrophe frequency (s^{-1})	0.033 ± 0.006	0.02 ± 0.003	0.014 ± 0.002	0.008 ± 0.003
(n)	(33)	(43)	(44)	(10)
Rescue frequency (s^{-1})	0.100 ± 0.019	0.085 ± 0.014	0.067 ± 0.011	0.145 ± 0.048
(n)	(27)	(36)	(39)	(9)
Dynamicity (dimers/sec)	147.0	113.1	45.0	23.5

BSC-1 cells were injected with rhodamine tubulin and incubated with the listed concentrations of nocodazole (Noc) for 1 h prior to observations of MTs. Velocities (mean ± SE), pauses, and transition frequencies (average ± SD) were calculated as described in MATERIALS AND METHODS.

Nocodazole also induces changes in the transition frequencies of dynamic instability (Tables 1 and 2). In newt lung cells perfused with nocodazole, catastrophe frequency increases approximately twofold, independent of concentration. Rescues were less frequent in the presence of nocodazole, with 4 nM nocodazole producing a threefold decrease in rescue. Interestingly, 100 nM and 400 nM nocodazole had less effect on rescue. Fewer rescues were observed in BSC-1 cells treated with 4 or 100 nM nocodazole, but rescue increased at 500 nM nocodazole; this latter effect may be due to an increase in the tubulin subunit pool. MTs in BSC-1 cells exhibited a dose-dependent decrease in catastrophe, by approximately fourfold at the highest concentration of nocodazole used. Thus, the major difference between the two cell types was the increase (newt lung cells) or decrease (BSC-1 cells) in catastrophe frequency. This difference was not due simply to the time of incubation in the drug since preliminary experiments with BSC-1 cells perfused with 100 nM nocodazole showed a similar catastrophe frequency (0.012 s^{-1}) compared with cells incubated for 1 h in nocodazole prior to observation (0.014 s^{-1}). It was not possible to follow MTs in newt lung cells incubated for 1 h with 100 nM nocodazole because all MTs at the peripheral regions of cells had depolymerized within 30–45 min (our unpublished observations).

The overall effect of nocodazole on dynamic instability can be summarized by calculating dynamicity, a measure of the gain and loss of subunits at MT ends per unit time (Toso *et al.*, 1993). For newt lung cells, dynamicity decreased at each nocodazole concentration examined with up to a twofold decrease at 400 nM nocodazole (Table 1). Similarly, BSC-1 cells showed a decrease in dynamicity, but the decrease was greater, with a sixfold decrease at 500 nM nocodazole (Table 2).

In both cell types, addition of nocodazole at 20–30 μM caused rapid depolymerization of the majority of MTs (our unpublished observations).

In Vitro MTs Assembled in Nanomolar Concentrations of Nocodazole Show Increases in Catastrophe Frequency and Time Spent in Pause

To further examine the effects of nocodazole on MT assembly, we used light microscopic assembly assays to follow the polymerization of phosphocellulose-purified tubulin nucleated from axoneme seeds. In initial experiments, tubulin and nocodazole were added directly to axoneme fragments, but MT assembly was slowed at both ends of the axoneme, making it impossible to differentiate the ends based on the rates of MT assembly (our unpublished observations). To distinguish plus and minus ends, individual MTs were followed before and after perfusion with nocodazole. For these studies, 12 μM purified tubulin, in assembly buffer containing excess GTP, was added to axoneme fragments and assembly was allowed to occur for several minutes at 35°C. A solution containing 12 μM tubulin (to prevent dilution-induced MT disassembly), GTP, and a given concentration of nocodazole (0, 4 nM, 100 nM, 400 nM, 1 μM, or 12 μM) was warmed briefly and perfused through the chamber, and MT assembly was followed for an additional 2 to 5 min. The rates of assembly preperfusion were used to classify ends as plus or minus. Life-history plots from representative plus-end MTs before and after 4 nM and 100 nM nocodazole perfusions are shown in Figure 3 and demonstrate the differences in MT behavior after addition of the drug. As shown in Figure 3, the changes in MT assembly were similar to those observed in vivo: the two-state behavior of dynamic instability was altered to include a third paused state with little length change over time, and

elongation and shortening velocities were reduced. Perfusion of 12 μM tubulin solutions lacking nocodazole did not effect dynamic instability (Figure 3A).

When individual parameters of dynamic instability were examined by pooling data at each nocodazole concentration, several alterations in dynamics were apparent. After perfusion with increasing concentrations of nocodazole, MT elongation velocity decreased at both plus and minus ends (Figure 4A). For plus ends, growth rates were reduced by 30% with 4 nM nocodazole and by 60% with nocodazole equimolar to the tubulin concentration. Minus-end elongation velocities were reduced to a slightly greater extent, ranging from 30% at 4 nM nocodazole to 80% at equimolar concentrations of the drug (Figure 4A). After perfusion with nocodazole, MT plus and minus ends also displayed a decrease in the velocity of rapid shortening (Figure 4B). For example, rapid shortening was reduced from 35.2 μm/min for plus ends in the absence of the drug to 20.6 μm/min after perfusion with 4 nM nocodazole and to 16.2 μm/min after perfusion with 1 μM nocodazole.

After nocodazole perfusion, MTs assembled in vitro were observed to spend a considerable percentage of time in a paused state. For plus ends, time spent in pause increases from 0% in control perfusions to ~40% after equimolar nocodazole perfusion (Figure 4C). For minus ends, the effect is more dramatic, with time spent in pause increasing from 0% for control perfusions to 95% after equimolar nocodazole perfusion (Figure 4C). These pauses were observed during rapid shortening and during elongation. MTs occasionally switched out of pause to growth or shortening; although these switches were rare, a switch to shortening was more likely. Because the number of switches was small, we did not calculate frequencies.

Nocodazole also alters catastrophe frequency at both plus and minus ends. For plus ends, catastrophe frequency increased approximately two- to threefold after perfusion with the different nocodazole concentrations studied (Figure 4D). At minus ends (Figure 4D), nanomolar concentrations of nocodazole caused a two- to fourfold increase in catastrophe frequency, whereas higher concentrations of nocodazole reduced the frequency of catastrophe. Thus, at low concentrations, nocodazole appears to act as a catastrophe promoter at both MT ends. Rescue frequency was also altered by nocodazole. As shown in Figure 4E, both plus and minus MT ends showed a decreasing probability of rescue as nocodazole concentration was increased. The one exception was seen at the plus ends, after treatment with 100 nM nocodazole; rescue increased slightly in this case.

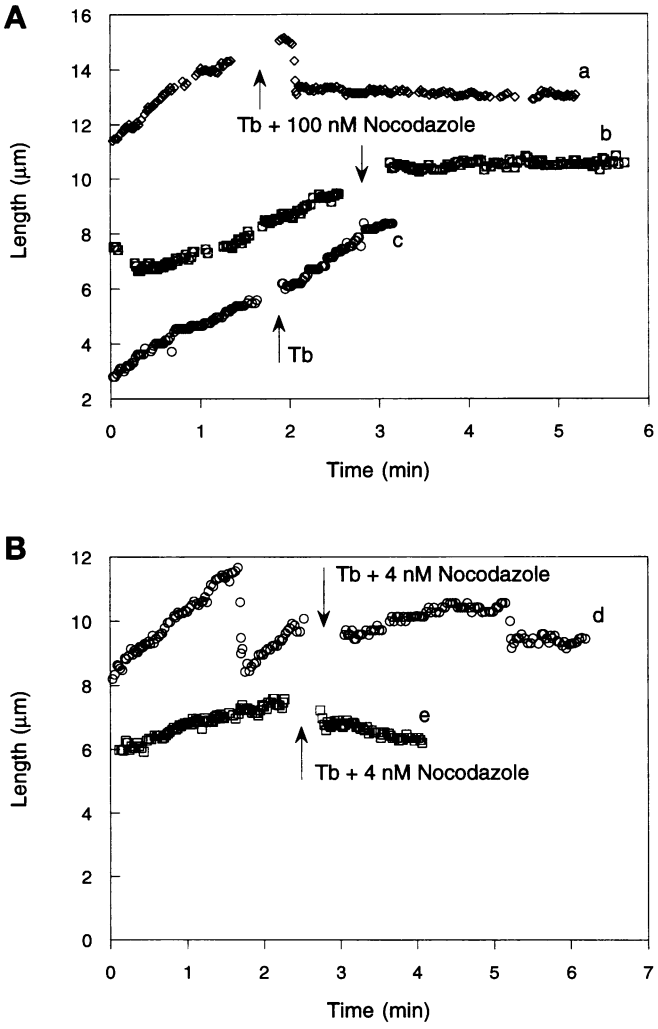

Figure 3. Life-history plots of plus-end MTs assembled in vitro from 12 μM tubulin and nucleated from axoneme fragments at 35°C. MTs are shown before and after perfusion with 12 μM tubulin, supplemented with 0, 4 nM, or 100 nM nocodazole. Perfusions are marked by arrows. Nocodazole addition at each concentration studied resulted in several possible changes in assembly: pauses in growth or shortening with little net length change (curves b and a, respectively), slower elongation (curve d), or slower shortening (curve e). Perfusion with 12 μM tubulin alone did not affect assembly (curve c).

Effects of Nocodazole on Axoneme-Seeded MT Nucleation and MT Resistance to Dilution Disassembly

Nocodazole could alter MT dynamics by binding to MT polymer or to tubulin dimers. To distinguish between the two mechanisms, we examined MT resistance to dilution-induced disassembly after nocodazole treatment. If, as is the case with vinblastine (Wilson *et al.*, 1982; Jordan *et al.*, 1991; Toso *et al.*, 1993), nocodazole binds to MTs and kinetically caps the MT end, then there should be an increase in resistance to

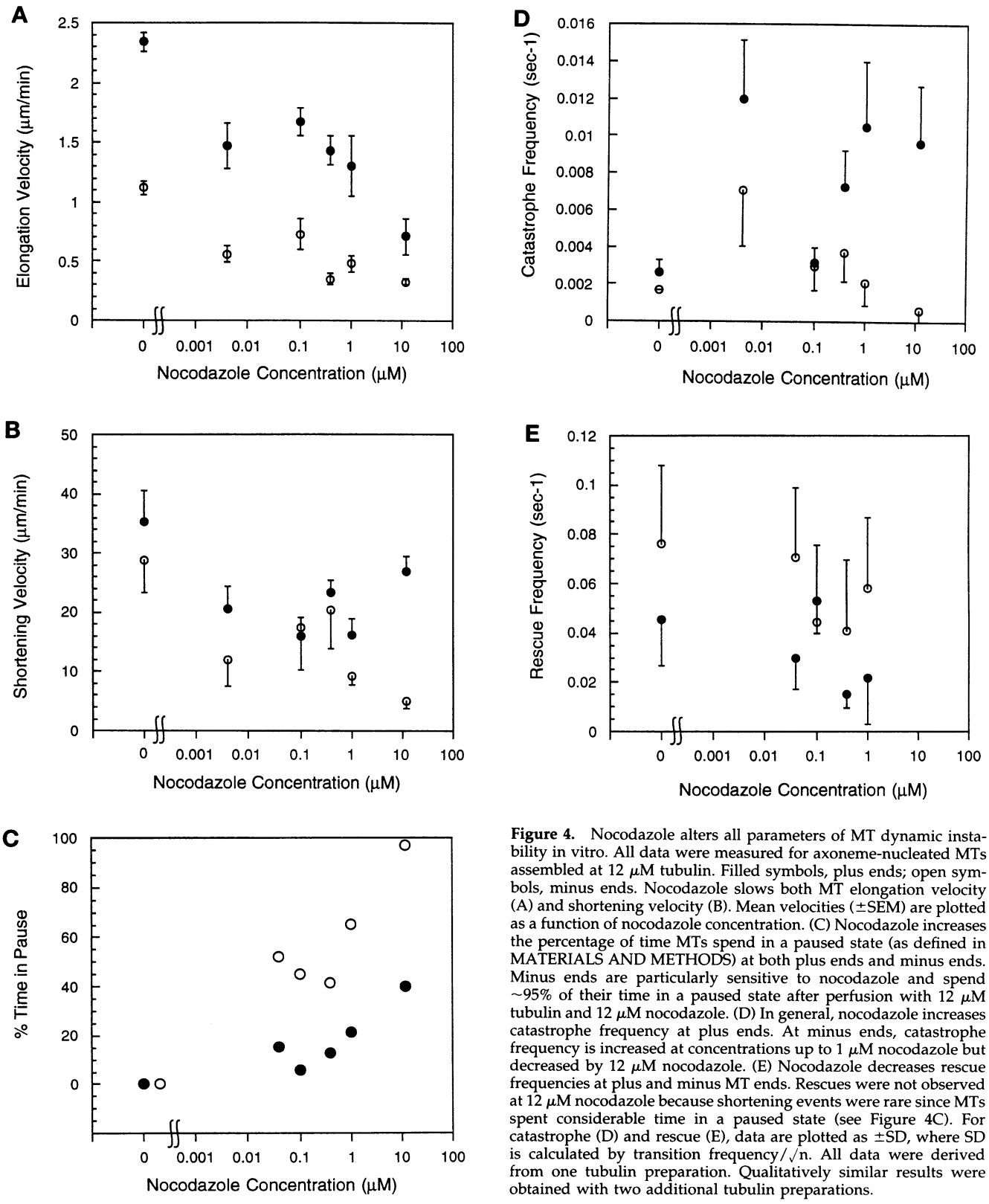

Figure 4. Nocodazole alters all parameters of MT dynamic instability in vitro. All data were measured for axoneme-nucleated MTs assembled at 12 μM tubulin. Filled symbols, plus ends; open symbols, minus ends. Nocodazole slows both MT elongation velocity (A) and shortening velocity (B). Mean velocities (±SEM) are plotted as a function of nocodazole concentration. (C) Nocodazole increases the percentage of time MTs spend in a paused state (as defined in MATERIALS AND METHODS) at both plus ends and minus ends. Minus ends are particularly sensitive to nocodazole and spend ~95% of their time in a paused state after perfusion with 12 μM tubulin and 12 μM nocodazole. (D) In general, nocodazole increases catastrophe frequency at plus ends. At minus ends, catastrophe frequency is increased at concentrations up to 1 μM nocodazole but decreased by 12 μM nocodazole. (E) Nocodazole decreases rescue frequencies at plus and minus MT ends. Rescues were not observed at 12 μM nocodazole because shortening events were rare since MTs spent considerable time in a paused state (see Figure 4C). For catastrophe (D) and rescue (E), data are plotted as ±SD, where SD is calculated by transition frequency/$\sqrt{n}$. All data were derived from one tubulin preparation. Qualitatively similar results were obtained with two additional tubulin preparations.

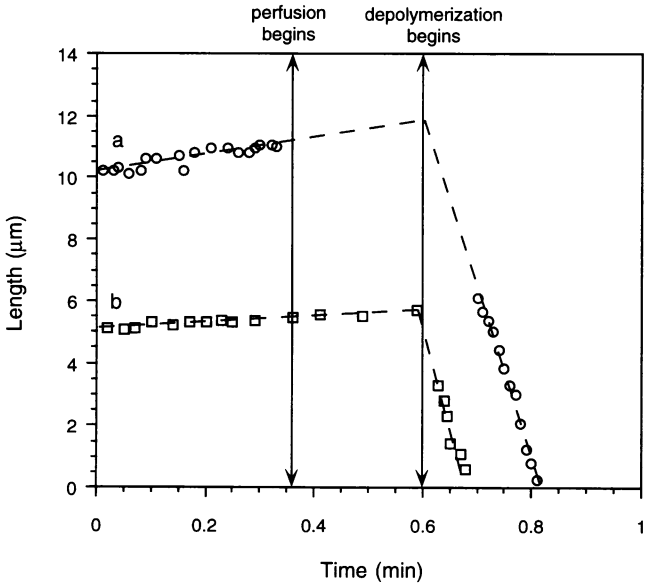

Figure 5. Nocodazole does not stabilize MTs to dilution-induced disassembly. MT plus-end lengths for an MT assembled from tubulin alone (curve a) and an MT assembled and then stabilized by perfusion with a tubulin solution containing 100 nM nocodazole (curve b) are shown. The first vertical line indicates the beginning of perfusion with PEM buffer. The second vertical line marks the onset of depolymerization for both MTs. These perfusions were conducted by two people (one to perfuse and one to focus) to maintain focus as much as possible during perfusion. The MT for curve a was out of focus for about 20 s, and the onset of depolymerization was determined by the intersection of lines through the assembly and disassembly portions of the curves. For MTs in curves a and b, depolymerization began about 14 s after perfusion. This is within the range of lag times, from perfusion to catastrophe, observed previously by Walker *et al.* (1991).

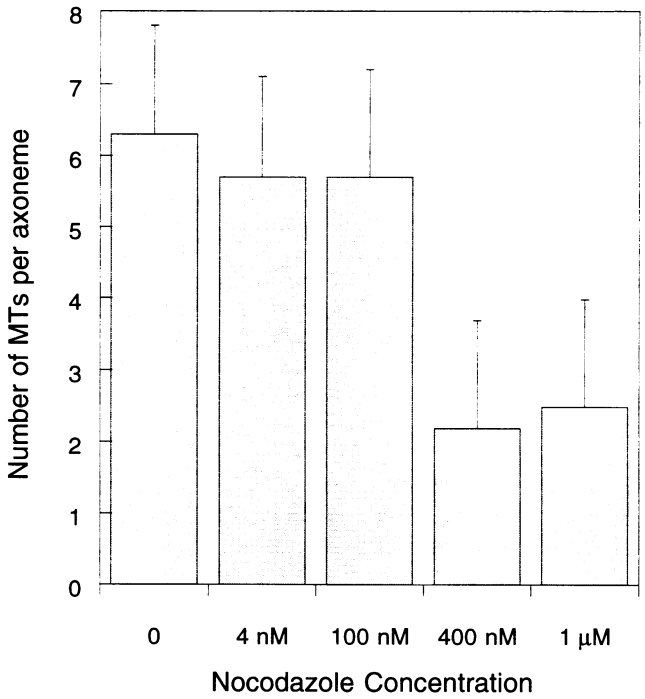

Figure 6. Nocodazole inhibits seeded nucleation from axoneme fragments. MTs were assembled in the presence of nocodazole for 5 to 10 min at 37°C and the number of MTs/axoneme were counted. Approximately 20 axonemes were examined at each concentration. Data are plotted as mean ± SD.

dilution-induced disassembly as a result of the reduced rate of tubulin dissociation. To test this possibility, 12 μM tubulin was assembled for several minutes prior to perfusion with 12 μM tubulin plus 100 nM or 1 μM nocodazole to stabilize MTs. After several minutes, the chambers were then perfused a second time with either buffer alone or buffer plus 100 nM or 1 μM nocodazole. MTs did not appear significantly stabilized by nocodazole, because the second perfusion resulted in the rapid shortening of all MTs observed, and this shortening occurred within the same time frame as observed with MTs not exposed to nocodazole (Figure 5). In fact, nearly all MTs had disappeared by the time focus was restored. Identical results were obtained whether or not the perfusion buffer contained GTP.

To determine whether nocodazole reduces axoneme-seeded MT nucleation, 12 μM tubulin was assembled from axonemes in the presence of 4 nM to 1 μM nocodazole at 35°C for 5 to 10 min. The number of MTs assembled from each axoneme end was counted 5–10 min after the start of assembly. In the controls, all of the 27 axonemes observed had MTs growing from both ends (mean number of MTs/axoneme end = 6.3). These results are similar to those obtained in previous experiments (Walker *et al.*, 1988). As shown in Figure 6, there was no significant change in the number of MTs nucleated/axoneme end in the presence of 4 or 100 nM nocodazole; however, assembly in 400 nM and 1 μM nocodazole resulted in dramatic decreases in the number of MTs/axoneme end. This decrease in number of MTs could result if assembly were too slow to allow MTs to reach measurable lengths during the assembly window. This is unlikely the case since assembly at rates as slow as 0.05–0.1 μm/min would be sufficient to generate a 0.25-μm MT in 5–10 min. At the higher nocodazole concentrations, many of the axonemes observed had MTs growing from one end only; however, the data from both ends were pooled, and no determination of the polarity of axonemes was made in these studies.

DISCUSSION

Nocodazole-induced Mitotic Arrest Is Likely Due to Suppression of MT Assembly Dynamics

Our observations demonstrate that substoichiometric concentrations of nocodazole, relative to tubulin, sup-

presses dynamic instability by decreasing MT elongation and shortening velocities both in vivo (Table 1 and 2) and in vitro (Figures 3 and 4), and by increasing the amount of time that MTs spend in a paused or attenuated state (Tables 1 and 2 and Figure 4C). Jordan *et al.* (1992) had previously demonstrated that nanomolar concentrations of nocodazole inhibited mitotic progression without significantly altering the MT polymer mass (Jordan *et al.*, 1992). The results presented herein suggest that the metaphase arrest observed with low concentrations of nocodazole results from MT stabilization. Several studies have also documented that low concentrations of vinblastine stabilizes MTs (Toso *et al.*, 1993; Dhamodharan *et al.*, 1995), and this treatment also causes mitotic arrest (Jordan *et al.*, 1992). Thus, these results suggest that suppression of dynamic instability can stall cells in mitosis, but it has not yet been determined whether these drugs also act on components of the spindle other than MTs. For example, it is possible that these drugs interfere with either kinetochore function or MT/kinetochore interactions. Consistent with this possibility, Wendell *et al.* (1993) found that kinetochore MT number was reduced by about 25% in cells arrested in mitosis by 2 nM vinblastine.

Nocodazole Alters the Two-State Behavior of Dynamic Instability To Include a Third Attenuated or Paused State

The most striking effect of nanomolar concentrations of nocodazole is to extend the amount of time MTs spend in an attenuated or paused state, with little or no detectable length changes over time, but the reactions at MT ends during a paused state are unknown. As discussed below, the nocodazole-induced paused state requires tubulin subunits in solution, suggesting that subunits continually add and subtract during this state. The attenuated state may represent a slowing down of tubulin subunit exchange at the MT end, as was proposed for vinblastine- and tubulin-colchicine complexes (reviewed in Wilson and Jordan, 1994). In support of this possibility, nocodazole caused significant decreases in the rates of growing and shortening both in vivo and in vitro. An alternative possibility is that the paused state may correspond to a kinetic or structural intermediate between growth and shortening as proposed by Walker *et al.* (1989). This intermediate was proposed based on the differential behavior of plus and minus ends after severing with a UV microbeam: minus ends continue to grow, whereas plus ends rapidly shorten (Walker *et al.*, 1989). The observation that minus ends spent a much greater percentage of time in a paused state than did plus ends (Figure 4C) is consistent with the inherent structural or kinetic differences between plus and minus ends.

Nanomolar Concentrations of Nocodazole Influence Catastrophe Frequency

In newt lung cells, low concentrations of nocodazole increase the catastrophe frequency approximately twofold (Table 1); however, catastrophe frequency was reduced in nocodazole-treated BSC-1 cells in a concentration-dependent manner (Table 2). This difference is unlikely a result of different incubation times in the drug since there was little difference in catastrophe frequency between BSC-1 cells perfused with nocodazole or incubated for 1 h in the drug. This suggests that the effects of nocodazole on catastrophe frequency are different in the two cell types examined. In untreated cells, the catastrophe frequency is likely the result of a combination of factors: local tubulin concentration, the activity of catastrophe promoters (Belmont and Mitchison, 1996; Walczak *et al.*, 1996), and stabilizing microtubule-associated proteins. The different effects of nocodazole in newt lung and BSC-1 cells may reflect a combined effect of nocodazole and these cellular factors. For example, in BSC-1 cells an increase in the tubulin subunit pool could offset any direct catastrophe-promoting activity of nocodazole.

In vitro, MT plus ends showed an approximately threefold increase in catastrophe frequency at nearly all nocodazole concentrations studied (Figure 4D). Minus ends also showed an increase in catastrophe frequency with 4 nM to 1 μM nocodazole, but a decrease at 12 μM nocodazole (Figure 4D). This latter decrease may result from the relatively large percentage of time these MTs spend in a paused state. In fact, when the time in pause is removed from the calculation of catastrophe, we calculate a threefold increase in the transition from growth to shortening compared with controls.

Overall, in both newt lung cells and in solutions of purified tubulin, nocodazole acts as a catastrophe promoter immediately after introduction of the drug. In both these systems, the nocodazole-induced increase in catastrophe frequency shows little concentration dependence (Table 1 and Figure 4D). If nocodazole increases catastrophe through an enzymatic mechanism (see below), then 4 nM nocodazole may be sufficient to generate a near maximal effect on catastrophe.

Two cellular catastrophe promoters have been identified recently, XKCM1 (Walczak *et al.*, 1996) and Op18/stathmin (Belmont and Mitchison, 1996). It is unlikely that nocodazole acts like XKCM1 (Walczak *et al.*, 1996), because XKCM1 is a kinesin-related protein that shows ATP-dependent binding to MTs but not tubulin dimers. However, nocodazole may share a similar mechanism of action with Op18/stathmin, a small heat-stable protein that interacts with tubulin dimers and promotes catastrophe (Belmont and Mitchison, 1996). At the present time, however, the

effects of Op18/stathmin on the rates of MT growth and shortening have not been analyzed in detail (Belmont and Mitchison, 1996).

The Effects of Nocodazole on MT Dynamics Are Likely Due to a Nocodazole-Tubulin Dimer Interaction and Formation of TuD Dimers

Our results demonstrate that a pool of tubulin subunits is necessary to maintain a paused state, supporting the view that nocodazole affects assembly through an interaction with tubulin dimers. Earlier studies with nocodazole indicate that it binds tubulin dimer and MT polymer (Lee *et al.*, 1980). Our observations do not call these findings into question, rather they indicate that the alterations in MT dynamics are likely mediated through a tubulin dimer-nocodazole interaction or a transient weak association with MT ends. This mechanism is different from that proposed for vinblastine. The effects of low concentrations of vinblastine on MT dynamics are believed to result from the binding of vinblastine to high-affinity sites at or near the growing end of the MT (Wilson *et al.*, 1982; Jordan and Wilson, 1990; Toso *et al.*, 1993; Dhamodharan *et al.*, 1995) and not on binding to the tubulin dimer. The mechanism of action of nocodazole may be more similar to colchicine whose effects on MT assembly are mediated by a tubulin-colchicine complex (Wilson and Farrell, 1986; Skoufias *et al.*, 1992). Unlike colchicine, however, the binding of nocodazole is rapidly reversible (Hoebeke *et al.*, 1976). Although the current data suggest that nocodazole effects MT dynamics through an interaction with tubulin dimers, a weak interaction with the MT end is not ruled out.

Previous studies have demonstrated that nocodazole increases the GTPase activity of pure tubulin by more than twofold and that unlike colchicine, no preincubation with tubulin is required to elicit this increase in activity (Lin and Hamel, 1981). More recent studies have demonstrated that nocodazole increases tubulin GTP hydrolysis by four- to fivefold and that this increase occurs in the absence of MT polymerization (Mejillano *et al.*, 1995). Currently, it is not known whether nocodazole remains bound to tubulin subunits after stimulating hydrolysis or whether it is released, allowing it to force hydrolysis on additional subunits. As shown recently by Vandecandelaere *et al.* (1995), small increases in the soluble pool of TuD subunits can significantly modulate MT dynamics. The results of Vandecandelaere *et al.* (1995) are strikingly similar to those observed herein and include pauses in assembly, reduced rates of elongation and shortening, and an increase in catastrophe frequency. These alterations in MT dynamics were observed at concentrations of TuD subunits that did not significantly alter the critical concentration for assembly (Vandecandelaere *et al.*, 1995). A recent study by Caplow and Shanks (1995) also found that an increase in the concentration of TuD subunits or generation of apotubulin subunits (tubulin that does not have a nucleotide bound in the exchangeable binding site, or E site), results in increased catastrophe frequency and decreased elongation velocity.

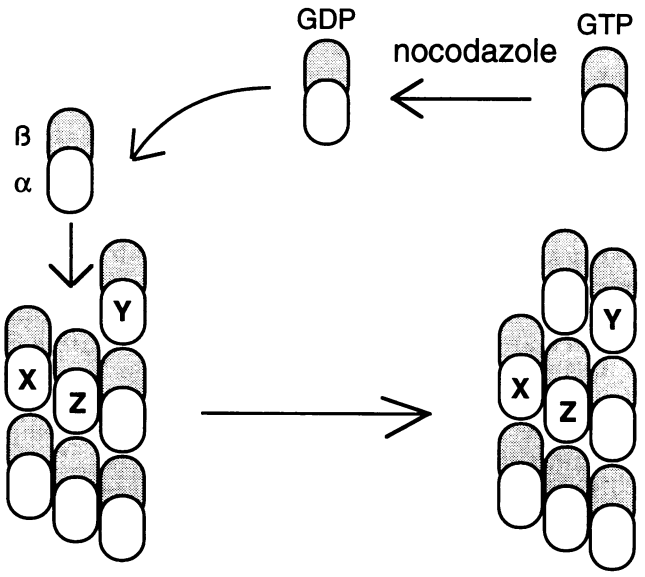

Figure 7. Model for MT assembly in the presence of nocodazole. This model is based on the lateral cap model of Bayley *et al.* (1990, 1994). Nocodazole stimulates the hydrolysis of GTP on the tubulin dimer leading to incorporation of TuD into the MT lattice. It is not known whether nocodazole remains bound to tubulin dimers after forcing hydrolysis. Addition of the incoming subunit to the MT end would force hydrolysis of GTP on subunit Z. The affinity of the incoming subunit for the MT end would depend on the GTP or GDP state of subunits X and Y, with highest affinity for two TuT subunits and lowest affinity for two TuD subunits. Addition of TuD, rather than TuT, results in an increased number of TuD/TuD or TuD/TuT sites and since these have lower affinity for the incoming subunit, elongation is slowed. The MT is shown with a B lattice and was redrawn after Vandecandelaere *et al.* (1995).

It is possible that nocodazole affects MT assembly by increasing tubulin GTPase activity. In this model, nocodazole binds to tubulin dimers, resulting in an increased rate of GTP hydrolysis and the formation of TuD subunits. This increased concentration of TuD subunits increases the likelihood of TuD incorporation at the MT ends. The nature of the nucleotide bound to adjacent subunits in the polymer then determines whether the MT continues to elongate (though more slowly), pauses, or undergoes a catastrophe (see Figure 7). Whether nocodazole significantly reduces GTP levels under our in vitro conditions is not known; however, significant changes in total GTP level would be surprising, given the excess of GTP typically present in in vitro assays. Overall GTP levels need not change though; rather, the concentration of TuD may increase, particularly if the rate of GDP release from

tubulin is slow in the presence of nocodazole. This type of model may have applications in vivo; cellular molecules that either speed up tubulin's GTP hydrolysis or inhibit GDP or Pi release could have dramatic effects on MT assembly in vivo, as suggested previously (Caplow, 1992).

A curious effect of nocodazole is the slowing of the shortening velocity, which appears incompatible with GTP-cap models and nocodazole action by simply generating TuD subunits (although slow shortening was also observed with increasing concentrations of TuD; Vandecandelaere *et al.*, 1995). For nocodazole, it is possible that weak interactions with the MT ends also contribute to slowing growth and shortening velocities, perhaps by mechanisms similar to vinblastine (Jordan *et al.*, 1986; Toso *et al.*, 1993).

The ability of nocodazole to rapidly enter cells and to rapidly bind tubulin makes it a useful probe for studying MT-based processes. It should be possible to study the role of dynamic MTs by slowing MT turnover in vivo with concentrations of nocodazole ≤100 nM.

ACKNOWLEDGMENTS

We are grateful to Jennifer Waters and Dr. Robert Hard for providing newts. R.J.V. and L.C. thank Drs. Ted Salmon, David Odde, and John Benbow for helpful discussions and Dr. Les Wilson for encouraging us to pursue these studies. Thanks also to Dr. Clare Waterman-Storer for critically reading the manuscript. Additional in vitro experiments, consistent with those presented herein, were performed with nocodazole synthesized by Dr. J. Benbow and we thank him for his generous gift of this product. Thanks also to Chris Patackis for help with MT tracking. R.J.V., B.H., and L.C. were supported by grants from the National Institutes of Health and the National Science Foundation. A.C.Y. and P.W. were supported by a grant from the National Science Foundation.

REFERENCES

Bayley, P.M., Schlistra, M.J., and Martin, S.R. (1990). Microtubule dynamic instability: numerical simulation of microtubule transition properties using a lateral cap model. J. Cell Sci. *95*, 33–48.

Bayley, P.M., Sharma, K.K., and Martin, S.R. (1994). Microtubule dynamics in vitro. In: Microtubules, ed. J.S. Hyams and C.W. Lloyd, New York: Wiley-Liss, 111–137.

Belmont, L., and Mitchison, T.J. (1996). Identification of a protein that interacts with tubulin dimers and increases the catastrophe rates of microtubules. Cell *84*, 623–631.

Caplow, M. (1992). Microtubule dynamics. Curr. Opin. Cell Biol. *4*, 58–65.

Caplow, M., and Shanks, J. (1995). Induction of microtubule catastrophe by formation of tubulin-GDP and apotubulin subunits at microtubule ends. Biochemistry *34*, 15732–15741.

Caplow, M., and Shanks, J. (1996). Evidence that a single monolayer of tubulin-GTP cap is both necessary and sufficient to stabilize microtubules. Mol. Biol. Cell *7*, 663–675.

Carlier, M.F., Didry, D., and Pantaloni, D. (1987). Microtubule elongation and guanosine 5′-triphosphate hydrolysis: role of guanine nucleotides in microtubule dynamics. Biochemistry *26*, 4428–4437.

Cassimeris, L. (1993). Regulation of dynamic instability. Cell Motil. Cytoskeleton *26*, 275–281.

Cassimeris, L., Pryer, N.K., and Salmon, E.D. (1988). Real-time observations of microtubule dynamic instability in living cells. J. Cell Biol. *107*, 2223–2231.

Cole, N., and Lippincott-Schwartz, J. (1995). Organization of organelles and membrane traffic by microtubules. Curr. Opin. Cell Biol. *7*, 55–64.

DeBrabander, M.J., Van De Veire, R.M.L., Aerts, F.E.M., Borgers, M., and Jannsen, P.A. (1976). The effects of methyl [5-(2-thienylcarbonyl)-1H-benzimidazol-2-yl] carbamate (R 17,943: NSC 238159), a new synthetic antitumoral drug interfering with microtubules, on mammalian cells cultured in vitro. Cancer Res. *36*, 905–916.

Drechsel, D.N., and Kirschner, M.W. (1994). The minimum GTP cap required to stabilize microtubules. Curr. Biol. *4*, 1053–1061.

Dhamodharan, R., Jordan, M.A., Thrower, D., Wilson, L., and Wadsworth, P. (1995). Vinblastine suppresses dynamics of individual microtubules in living interphase cells. Mol. Biol. Cell *6*, 1215–1229.

Dhamodharan, R., and Wadsworth, P. (1995). Modulation of microtubule dynamic instability in vivo by brain microtubule associated proteins. J. Cell Sci. *108*, 1679–1689.

Erickson, H.P., and O'Brien, E.T. (1992). Microtubule dynamic instability and GTP hydrolysis. Annu. Rev. Biophys. Biomol. Struct. *21*, 145–166.

Friedman P.A., and Platzer, E.G. (1978). Interaction of antihelmintic benzimidazoles and benzimidazole derivatives with bovine brain tubulin. Biochim. Biophys. Acta *544*, 605–614.

Gliksman, N., Parsons, S.F., and Salmon, E.D. (1992). Okadaic acid induces interphase to mitotic-like microtubule dynamic instability by inactivating rescue. J. Cell Biol. *119*, 1271–1276.

Hoebeke, J., Van Nijen, G., and DeBrabander, M. (1976). Interactions of oncodazole (R 17934), a new anti-tumoral drug, with rat brain tubulin. Biochem. Biophys. Res. Commun. *69*, 319–324.

Hyman, A., Drechsel, D., Kellogg, Salser, D., S., Sawin, K., Steffen, P., Wordeman, L., and Mitchison, T. (1991). Preparation of modified tubulins. Methods Enzymol. *196*, 478–485.

Hyman, A.A., Salser, S., Drechsel, D.N., Unwin, N., and Mitchison, T.J. (1992). Role of GTP hydrolysis in microtubule dynamics: information from a slowly hydrolyzable analogue, GMPCPP. Mol. Biol. Cell *3*, 1155–1167.

Inoue, S., and Salmon, E.D. (1995). Force generation by microtubule assembly/disassembly in mitosis and related movements. Mol. Biol. Cell *6*, 1619–1640.

Ireland, C.M., Gull, K., Gutteridge, W.E., and Pogson, C.I. (1979). The interaction of benzimidazole carbamates with mammalian microtubule protein. Biochem. Pharmacol. *28*, 2680–2682.

Jordan, M.A., Margolis, R.L., Himes, R.H., and Wilson, L. (1986). Identification of a distinct class of vinblastine binding sites on microtubules. J. Mol. Biol. *187*, 61–73.

Jordan, M.A., Thrower, D., and Wilson, L. (1991). Mechanism of inhibition of cell proliferation by the *Vinca* alkaloids. Cancer Res. *51*, 2212–2222.

Jordan, M.A., Thrower, D., and Wilson, L. (1992). Effects of vinblastine, podophyllotoxin and nocodazole on mitotic spindles: implications for the role of microtubule dynamics in mitosis. J. Cell Sci. *102*, 401–416.

Jordan M.A., Toso, R.J., Thrower, D., and Wilson, L. (1993). Mechanism of mitotic block and inhibition of cell proliferation by Taxol at low concentrations. Proc. Natl. Acad. Sci. USA *90*, 9552–9556.

Jordan, M.A., and Wilson, L. (1990). Kinetic analysis of tubulin exchange at microtubule ends at low vinblastine concentrations. Biochemistry *29*, 2730–2739.

Lee, J.C., Field, D.J., and Lee, L.L.Y. (1980). Effects of nocodazole on the structures of calf brain tubulin. Biochemistry *19*, 6209–6215.

Lin, C.M., and Hamel, E. (1981). Effects of inhibitors of tubulin polymerization on GTP hydrolysis. J. Biol. Chem. *256*, 9242–9245.

Mejillano, M.R., Shivanna, B.D., and Himes, R.H. (1995). The GTPase activity of tubulin. Mol. Biol. Cell *6*, 258a (Abstract).

Melki, R., Carlier, M.F., and Pantaloni, D. (1990). Direct evidence for GTP and GDP-Pi intermediates in microtubule assembly. Biochemistry *29*, 8921–8932.

Mitchison, T., and Kirschner, M.W. (1984a). Microtubule assembly nucleated by isolated centrosomes. Nature *312*, 232–237.

Mitchison, T., and Kirschner, M. (1984b). Dynamic instability of microtubule growth. Nature *312*, 237–242.

Morrisey, J.H. (1981). Silver stain for proteins in polyacrylanide gels: a modified procedure with enhanced sensitivity. Anal. Biochem. *117*, 307–310.

Rose, G.G., Pomerat, C.M., Shindler, T.O., and Trunnell, J.B. (1958). A cellophane-strip technique for culturing tissue in multipurpose chambers. J. Biophys. Biochem. Cytol. *4*, 761–764.

Shelden, E., and Wadsworth, P. (1993). Observation and quantification of individual microtubule behavior in vivo: microtubule dynamics are cell-type specific. J. Cell Biol. *120*, 935–945.

Skoufias, D., and Wilson, L. (1992). Mechanism of inhibition of microtubule polymerization by colchicine: inhibitory potencies of unliganded colchicine and tubulin-colchicine complexes. Biochemistry *31*, 738–746.

Tanaka, E., Ho, T., and Kirschner, M. (1995). The role of microtubule dynamics in growth cone motility and axonal growth. J. Cell Biol. *128*, 139–155.

Taylor, J.R. (1982). An Introduction to Error Analysis, Mill Valley, CA: University Science Books, 207–217.

Toso, R.J., Jordan, M.A., Farrell, K.W., Matsumoto, B., and Wilson, L. (1993). Kinetic stabilization of microtubule dynamic instability in vitro by vinblastine. Biochemistry *32*, 1285–1293.

Vasquez, R.J., Gard, D.L., and Cassimeris, L. (1994). XMAP from *Xenopus* eggs promote rapid plus end assembly of microtubules and rapid microtubule polymer turnover. J. Cell Biol. *127*, 985–993.

Vandecandelaere, A., Martin, S.R., and Bayley, P.M. (1995). Regulation of microtubule dynamic instability by tubulin-GTP. Biochemistry *34*, 1332–1343.

Vigers, G.P., Coue M., and McIntosh, J.R. (1988). Fluorescent microtubules break up under illumination. J. Cell Biol. *107*, 1011–1024.

Wadsworth, P., and Salmon, E.D. (1986). Preparation and characterization of fluorescent analogs of tubulin. Methods Enzymol. *134*, 519–528.

Walczak, C.E., Mitchison, T.J., and Desai, A. (1996). XKCM1: a *Xenopus* kinesin-related protein that regulates microtubule dynamics during mitotic spindle assembly. Cell *84*, 37–47.

Walker, R.A., Inoue, S., and Salmon, E.D. (1989). Asymmetric behavior of severed microtubules following ultraviolet-microbeam irradiation of individual microtubules in vitro. J. Cell Biol. *108*, 931–937.

Walker, R.A., O'Brien, E.T., Pryer, N.K., Soboeiro, M.F., Voter, W.A., Erickson, H.P., and Salmon, E.D. (1988). Dynamic instability of individual, MAP-free microtubules analyzed by video light microscopy: rate constants and transition frequencies. J. Cell Biol. *107*, 1437–1448.

Walker, R.A., Pryer, N.K., and Salmon, E.D. (1991). Dilution of individual microtubules observed in real time in vitro: evidence that cap size is small and independent of elongation rate. J. Cell Biol. *114*, 73–81.

Wendell, K.L, Wilson, L., and Jordan, M.A. (1993). Mitotic block in HeLa cells by vinblastine: ultrastructural changes in kinetochore-microtubule attachment and in centrosomes. J. Cell Sci. *104*, 261–274.

Wilson, L., and Farrell, K.W. (1986). Kinetics and steady-state dynamics of tubulin addition and loss at opposite microtubule ends: the mechanism of action of colchicine. Ann. NY Acad. Sci. *466*, 690–708.

Wilson, L., and Jordan, M.A. (1994). Pharmacological probes of microtubule function. In: Microtubules, ed. J.S. Hyams and C.W. Lloyd, New York: Wiley-Liss, 59–83.

Wilson, L., and Jordan, M.A. (1995). Microtubule dynamics: taking aim at a moving target. Chem. Biol. *2*, 569–573.

Wilson, L., Jordan, M.A., Morse, A., and Margolis, R.L. (1982). Interaction of vinblastine with steady-state microtubules in vitro. J. Mol. Biol. *159*, 129–149.